

# THERMAL DECOMPOSITION OF VEGETATIVE FUELS

Isaac T. Leventon<sup>A</sup> and Morgan C. Bruns<sup>B</sup>

<sup>A</sup> *National Institute of Standards and Technology, Fire Research Division,  
100 Bureau Drive; Building 224, Room A265; Gaithersburg, MD, 20899; United States*

<sup>B</sup> *Virginia Military Institute, Department of Mechanical Engineering  
710 Nichols Hall; Lexington, VA 24450; United States*

## ABSTRACT

This manuscript presents new measurement data from milligram-scale thermal decomposition experiments - thermogravimetric analysis (TGA) and microscale combustion calorimetry (MCC) – conducted on stems and leaves of six plant species commonly found across the United States. For each fuel, measurement data from TGA experiments was analyzed to determine effective thermal decomposition mechanisms and the associated kinetics of their constituent reactions. MCC experiments were repeated under identical experimental conditions to determine the heats of complete combustion of all gaseous volatiles produced by these vegetative fuels and to validate the decomposition mechanisms and species char yields determined from TGA data. Through a coupled analysis of TGA and MCC measurement data, an estimate of the heats of combustion of the gaseous volatiles produced by individual reaction steps in the fuel's decomposition was also made. Between different fuels, distinct differences were measured in the onset temperature of decomposition, the temperature range of decomposition, the number of apparent reactions, and the peak measured mass loss and heat release rates (as well as the temperatures at which they occur). To analyze the impact of these variations on predictions of wildfire behavior, a modeling study was then conducted in which simulations of wildland fire experiments were repeated using the thermal decomposition mechanisms and heats of combustion determined for six of the fuel species tested in this work. Model-predicted fire spread rate in these simulations varied between  $0.50 \text{ m s}^{-1}$  and  $1.09 \text{ m s}^{-1}$ .

## INTRODUCTION

With a growing number of people moving to areas in or near fire prone wildlands<sup>1</sup> and an increase in the number of large fires and total acres burned each year<sup>2</sup>, wildland fires are an increasingly dangerous and costly problem. Accurate predictive modeling of current (or potential) uncontrolled wildland fires (i.e., quantitative prediction of fire intensity and spread rate) can mitigate the risk that these fires pose. Common models of wildland fire spread (e.g., BehavePlus<sup>3</sup> and FARSITE<sup>4</sup>) are relatively easy to use and can quickly provide fire spread predictions and deterministic assessments of fire hazard; however, they are based upon empirical relations (e.g., Rothermel<sup>5</sup>) defining a constant rate of spread for given conditions of slope, weather, wind, moisture, and a user-selected fuel model. These fuel models define representative physical parameters (surface area to volume ratio, particle size, and fuel bed depth), moisture content, and heat content (prescribed as  $18.6 \text{ kJ g}^{-1}$  for all but one, of 40 available, fuel models)<sup>6</sup>. Such empirically based models of flame spread have valuable applications (e.g., they are used for operational predictions of flame spread rate) but they do not incorporate the underlying processes controlling wildland fire spread behavior<sup>7</sup>. Thus, they are unable to predict transient fire behaviors and they may not be able to provide accurate predictions of fire behavior under changing ambient conditions or when a mixture of fuel sources (vegetative and structural) is present (e.g., at the wildland urban interface, WUI).

More powerful physics-based models (e.g., FDS<sup>8</sup>) can better capture the controlling mechanisms of wildland fires by solving governing equations for buoyant flow, heat and mass transfer, gas phase

combustion, and condensed phase thermal decomposition of fuels. These more capable simulation tools may be particularly valuable at the WUI, where simulation of the burning behavior of vegetative and structural fuels could be used to better inform structural and community wildfire resilience. Such models require a large number of inputs (e.g., fuel heat of combustion and radiative fraction, thermophysical properties of the vegetation and soil, and ambient conditions) to provide accurate predictions of wildland fire behavior. It has been shown that model predictions of the rate of spread of wildland fires are particularly sensitive to windspeed and the thermal decomposition temperature of the burning vegetative fuel<sup>9</sup>. Unfortunately, despite this sensitivity, comprehensive measurements of thermal decomposition are not readily available for a variety of common vegetative fuels and the fuel properties that are available from such experiments (i.e., the relevant data needed to parameterize physics-based models of wildfire spread) can be subject to large uncertainties<sup>10</sup>.

Philpot conducted an early study on the pyrolysis of plant materials, using thermogravimetric analysis (TGA) and differential thermal analysis (DTA), to examine the relationship between a plant's mineral content and pyrolysis behavior (rate, onset temperature, and residue yields)<sup>11</sup>. Shafizadeh presented a thorough review of the pyrolysis of biomass, that described how the composition of its major components (cellulose, hemicellulose, and lignin) impacts its thermal properties and available decomposition pathways and that quantified the species yields of decomposition reactions how these vary with pyrolysis temperature<sup>12</sup>. Through the 1980s, Sussot led a series of studies on a broad range of wildland fuels, identifying the temperature range of decomposition for various plant components, the total heat needed for their pyrolysis, and the total energy released by combustion of these gaseous pyrolyzates (using an experimental apparatus that was a precursor to modern microscale combustion calorimetry)<sup>13-16</sup>. TGA experiments were also performed on multiple Mediterranean plant species to provide a ranking of their 'potential combustibility'<sup>17</sup> and other authors have thoroughly studied individual fuels (and their gaseous pyrolyzates) using multiple analytical methods<sup>18</sup>. Most recently, Amini and Safdari have characterized the char, tar, and gaseous species yields, and their respective chemical compositions, of the pyrolysis products of (live and dead samples of) fifteen species of vegetation native to the Southern United States<sup>19,20</sup>.

This manuscript presents new measurements from milligram-scale thermal decomposition experiments - thermogravimetric analysis (TGA) and microscale combustion calorimetry (MCC) – conducted on stems and leaves of six plant species commonly found in the United States. These fuels were collected in the summer of 2017 by the US Forest Service in Missoula, Montana (Lodgepole Pine, and Douglas-Fir) and in the North Mountain experimental area in Southern California (Chamise, Bigberry Manzanita, Desert Ceanothus, and Chaparral Whitethorn). All tests were conducted in nitrogen (i.e., in an anaerobic environment). Although the rate of degradation of these fuels may be affected by oxidation, it has been noted<sup>21</sup> that thin vegetative fuels will not ignite by pure radiative heating thus convective heating and flame 'bathing' is critical. Such direct flame impingement presents a 'fuel rich' (and thus a largely anaerobic) environment at the fuel's surface as it pyrolyzes.

For each fuel, sample mass and mass loss rate measured in TGA experiments were analyzed to determine effective thermal decomposition mechanisms and associated kinetics of these reactions. MCC experiments were repeated under the same experimental conditions to determine the heats of complete combustion of all gaseous pyrolyzates and species char yields. Additionally, by a coupled analysis of TGA and MCC measurement data, an estimate of the heats of combustion of the gaseous volatiles produced by individual reaction steps was made. To analyze the impact of variations in the degradation behavior of these fuels, a study was then conducted in which simulations of grassland fire experiments<sup>8,9</sup> were repeated using the unique thermal decomposition mechanisms and heats of combustion determined in this work. The sensitivity of model-predicted development of fire spread rate to these variations is discussed.

## **MATERIALS AND METHODS**

### **Materials**

The vegetative fuels studied in this work were obtained between May and July of 2017 from the United States Forest Service Pacific Southwest and Rocky Mountain Research Stations (which are located in Southern California and Western Montana, respectively). Species locations of origin,

scientific names, and common names are provided in Table 1. The selected species represent vegetation types commonly found in the regions in which they were picked. For each species, a bulk sample – consisting of small branches with leaves attached – was picked from a series of randomly selected individual plants. Milligram-scale experiments conducted in this work were performed on both leaves and stems of all six plant species (except for Douglas-fir) thus creating a test matrix of eleven unique fuel species. Thermal analysis experiments were conducted on Douglas-fir leaves only.

Table 1. Vegetative fuels tested in this study

Origin	Scientific Name	Common Name
Pacific Southwest Research Station (North Mountain Experimental Area, California)	Adenostoma Fasciculatum	Chamise
	Arctostaphylos Glauca	Bigberry Manzanita
	Ceanothus Greggii	Desert Ceanothus
	Ceanothus Leucodermis	Chaparral Whitethorn
Rocky Mountain Research Station (Missoula, Montana)	Pinus Contorta	Lodgepole Pine
	Pseudotsuga Menziesii	Douglas-Fir

A preliminary series of TGA experiments was conducted on samples in one of two states: fresh (tested within 1-2 weeks after being picked) and after being microwaved three times (60 s each), sealed in plastic sample bags, and stored in a refrigerator. This treatment ensured the stability of samples (i.e., prevented decay, degradation, and/or molding) without affecting the chemical or physical structure of the foliage. Differences in measured sample mass and mass loss rate (MLR) of fresh and microwaved samples during these TGA experiments were negligible, thus all experimental measurements presented in this work were performed on samples that had been microwaved.

After this treatment, samples were cut into thin (< 0.75 mm thick) flat sections, less than 5 mm in length and between 4.5 mg – 6.5 mg in mass. For each test, leaves were kept whole/intact and stems were cut through their middle to create a flat surface that allowed for good thermal contact during experiments. All samples were stored in a desiccator (in the presence of Drierite) for a minimum of 48 hours prior to testing. Immediately before testing, samples were removed from the desiccator, pressed flat into the base of alumina test crucibles, and weighed using a Mettler M3 analytical balance.

### Thermal Analysis Experiments

Thermogravimetric Analysis (TGA) experiments were conducted in a Netzsch STA 449 F1 Jupiter. This apparatus continuously measures mass (using a microbalance with a 0.025 µg precision) and temperature (using an S-type thermocouple positioned directly beneath the sample crucible) of samples as they are heated through a well-defined temperature program in an anaerobic environment. A temperature calibration was conducted as per the manufacturer's recommendations<sup>22</sup> - using a set of 6 pure metals, with melting points between 156.6 °C and 961.8 °C - to provide a relation between measured and actual sample temperature. The calibration was performed using the same crucible type, heating rate, and gaseous environment as was used during thermal analysis experiments on vegetative fuel samples. All TGA experiments were conducted within three months of this calibration.

The temperature program used for TGA experiments included an initial heating at 10 °C min<sup>-1</sup> to 75 °C followed by a 20-minute-long isotherm at that temperature, during which time the chamber was continuously purged with nitrogen. This conditioning period ensured that the system was completely free of oxygen and that any residual moisture in samples was removed prior to dynamic heating and thermal decomposition. Following this conditioning period, samples were heated at a constant rate of 10 °C min<sup>-1</sup> to 700 °C (approximately 200 °C above the highest temperature at which a mass loss event was observed). Throughout this program, the test chamber was continuously purged with ultra-high purity (UHP) nitrogen at 50 mL min<sup>-1</sup> to ensure thermal decomposition of samples occurred without oxidation. All tests were conducted in open alumina crucibles to allow gaseous pyrolyzates to escape unimpeded.

At the start of each day of testing, a baseline test was performed in which an empty alumina crucible was subjected to the same heating program as was used during thermal analysis experiments. This

baseline history (mass vs. temperature) was subtracted from the corresponding data obtained during experiments on vegetative fuel samples; all TGA measurement data presented in this work has been baseline-corrected in this manner. For each test, measured sample mass,  $m$ , was normalized by initial sample mass,  $m_0$ . Normalized sample mass loss rate  $\frac{d(m/m_0)}{dt}$  [s<sup>-1</sup>] was calculated as the numerical derivative of time-resolved sample mass curves and, prior to further analysis, noise in mass loss rate curves was reduced using a Savitzky-Golay filter. For each fuel species and sample type (stem and leaf), tests were repeated five times to accumulate necessary statistics; mass history curves from repeated experiments were averaged together prior to further analysis.

The relatively low heating rate (10 °C min<sup>-1</sup>) used in these experiments was selected, in combination with the small sample masses used during testing, to ensure that samples did not experience significant temperature or composition gradients during heating<sup>23,24</sup>. Further, it has been demonstrated that an inverse analysis of total mass and mass loss rate data measured in TGA experiments conducted under these conditions can be used to determine effective reaction mechanisms, and associated reaction kinetics, that accurately describe the thermal decomposition of combustible solids<sup>25</sup>.

Effective reaction mechanisms for all fuels were calculated assuming that measured decomposition behavior could be captured by a series of parallel, first order, Arrhenius rate reactions of the form

$$\frac{dm}{dt} = -\sum_i(1 - v_i)m_iA_i \exp\left(\frac{E_i}{RT}\right) \quad [1]$$

where  $m$  is the total sample mass,  $m_i$  is the mass of component  $i$ ,  $T$  is the sample temperature,  $R$  is the gas constant, and  $A_i$  and  $E_i$  are the kinetic parameters describing the reaction. Assuming a parallel reaction mechanism is reasonable in this case since it is likely that the vegetative fuels are composed of distinct components (cellulose, hemicellulose, and lignin)<sup>12, 14</sup>. TGA data does not allow for the determination of either the stoichiometric coefficient,  $v_i$ , or the initial amount of component  $i$  present in the material,  $m_{0,i}$ . However, it is possible to determine the amount of mass lost as volatiles in each reaction from the TGA data. This quantity is simply  $\Delta m_i \equiv m_{0,i}(1 - v_i)$ . The solid residue yield is related to the reaction mass losses through  $\mu = 1 - \sum_i \Delta m_i$ . For each of the fuels considered, the kinetic parameters  $A_i$  and  $E_i$  along with the reaction mass losses,  $\Delta m_i$  were determined using the algorithm developed in a recent work<sup>26</sup>.

Microscale Combustion Calorimetry (MCC) experiments were conducted in an apparatus built in accordance with the relevant standard, ASTM D7309<sup>27</sup>. In this test, specimens of known mass are thermally decomposed in an anaerobic environment at a constant heating rate. Gaseous volatiles released by pyrolyzing samples are mixed with an inert carrier gas and transported to a high temperature combustion chamber where they are forced to complete combustion in an oxygen rich environment. The heat released by combustion of these volatiles is computed from the rate of oxygen consumption in the gas stream exiting the combustion furnace. Sample temperature is continuously monitored during tests using a K-type thermocouple positioned directly beneath the sample crucible.

A temperature calibration was conducted as per best practices<sup>27, 28</sup> to provide a relation between measured and actual sample temperature. The calibration was performed using the same crucible type, heating rate, and gaseous environment as was used during thermal analysis experiments on vegetative fuel samples. All MCC tests were conducted within three months of this calibration. At the start of each day of testing, the MCC oxygen sensor was calibrated using a prepared gas mixture (19.19 % oxygen in nitrogen) and the total system calibration was checked using a reference material, polystyrene (Styron 665 GP). MCC experiments were conducted in accordance with ASTM D7309<sup>27</sup> using 4.5 mg to 6.5 mg material samples that were pyrolyzed in UHP nitrogen. Samples were placed into open alumina crucibles, introduced into the pyrolysis chamber, and allowed to reach equilibrium at a temperature of 75 °C, at which point the chamber temperature was increased to 700 °C at a constant heating rate of 10 °C min<sup>-1</sup>. Although the standard<sup>27</sup> recommends heating rates between 12 °C min<sup>-1</sup> and 120 °C min<sup>-1</sup>, a heating rate of 10 °C min<sup>-1</sup> was selected in this study to provide measurements of sample heat release rate under comparable conditions to those used in TGA experiments.

The heat of complete combustion of all gaseous pyrolyzates ( $\Delta H_{c,total}$ ) released by the pyrolyzing sample was determined as the integral of heat release rate, HRR, measured throughout the duration of tests divided by final volatilized mass,  $m_{vol}$  (i.e., initial sample mass minus the mass of char remaining after each test:  $m_{vol} = m_0 - m_{char}$ ). Char yield,  $\mu_{char}$ , was calculated by dividing  $m_{char}$  by  $m_0$ . Each fuel species was tested in the MCC at least three times to ensure reproducibility;  $\Delta H_{c,total}$  and  $\mu_{char}$  were calculated for each repeated experiment to accumulate necessary statistics. Values of  $\Delta H_{c,total}$  and  $\mu_{char}$  reported in this manuscript represent average values of repeated measurements.

Heats of complete combustion of the gases species produced during each reaction step,  $\Delta H_{c,i}$ , were determined by comparing heat release rate measured in MCC experiments and mass loss rate predicted by the decomposition model (which was developed on the basis on TGA experiments). The model was used to simulate sample mass loss rate under the conditions matching TGA and MCC experiments and a predicted heat release rate curve was generated by scaling the instantaneous rate of gaseous volatile production attributed to each reaction step by its corresponding  $\Delta H_{c,i}$ . These heats of combustion were adjusted in an iterative process until acceptable agreement between model-predicted and experimentally-measured heat release rate was obtained.

### Numerical Simulations of Wildfire Spread

Computational Fluid Dynamics (CFD) simulations of wildfire spread were conducted in the NIST Fire Dynamics Simulator (FDS version 6.7.1)<sup>29</sup> to determine the sensitivity of flame spread rate predictions to measured variations in fuel decomposition behavior. Selected as a case study for this sensitivity analysis was a controlled burn of a 100 m by 100 m plot of kerosene grasslands conducted by the Commonwealth Scientific and Industrial Research Organization (CSIRO) of Australia between July and August of 1986 (Case C064)<sup>30</sup>. Measured properties of this case are reported in Table 2.

Table 2. Measured properties of CSIRO Grassland Fire Case C064<sup>30</sup>

Property	Value
Wind Speed	4.6 m s <sup>-1</sup>
Ambient Temperature	32 °C
Surface Area to Volume Ratio	9770 m <sup>-1</sup>
Grass Height	0.21 m
Bulk Mass per Unit Area	0.283 kg m <sup>-2</sup>
Moisture Fraction	6.3%

The computational domain in this case is 120 m by 120 m by 20 m. This domain is subdivided into 36 meshes, each with 0.5 m cubic grid cells. Increasing or decreasing grid size by a factor of 2 yields approximately a 5% deviation in model-predicted flame spread rate. In these simulations, Lagrangian particles are used to simulate blades of grass, which are modeled as slender cylinders whose diameters are inferred from the measured surface area to volume ratio. Each grid cell contains one simulated blade of grass; by applying a weighting factor, each explicitly modeled blade of grass represents approximately 5000 actual blades, thus matching the experimentally measured bulk mass per unit area. Blades of grass are rigidly fixed, perpendicular to the wind and the source of thermal radiation. Further detail on model assumptions concerning heat transfer and drag around blades of grass is provided elsewhere<sup>9</sup>.

Wildfire simulations were repeated using the reaction mechanisms and associated kinetics and heats of combustion determined for six of the vegetative fuels tested in this work. Two additional simulations were also defined using decomposition models that represent the degradation of a typical leaf or stem; these models are referred to as ‘Average Leaf’ and ‘Average Stem’. These cases provide insight into whether a given vegetative fuel’s degradation mechanism can be estimated (based on existing knowledge) or if it must be uniquely measured to provide reasonable predictions of wildfire spread. Requisite parameters defining these decomposition models are reported, in further detail, in the ‘Results and Discussion’ section of this manuscript. All other relevant soil, vegetation, and combustion parameters used in these simulations are reported in Table 3; these values have been taken from a recent modeling study<sup>9</sup> and are typical of wood or cellulosic fuels. Ignition was defined to match experimental conditions, as described in a recent work<sup>9</sup>.

Table 3. Assumed Fuel and Soil Properties for Wildfire Simulations <sup>9</sup>

Property	Value
Fuel Properties	
Chemical Composition	C <sub>6</sub> H <sub>10</sub> O <sub>5</sub>
Radiative Fraction	0.35
Soot Yield	0.015
Specific Heat	1.5 kJ kg <sup>-1</sup> K <sup>-1</sup>
Conductivity	0.1 W m <sup>-1</sup> K <sup>-1</sup>
Density	512 kg m <sup>-3</sup>
Heat of Pyrolysis	418 kJ kg <sup>-1</sup>
Soil Properties	
Soil Specific Heat	2.0 kg <sup>-1</sup> K <sup>-1</sup>
Soil Conductivity	0.25 W m <sup>-1</sup> K <sup>-1</sup>
Soil Density	1300 kg m <sup>-3</sup>

## RESULTS AND DISCUSSION

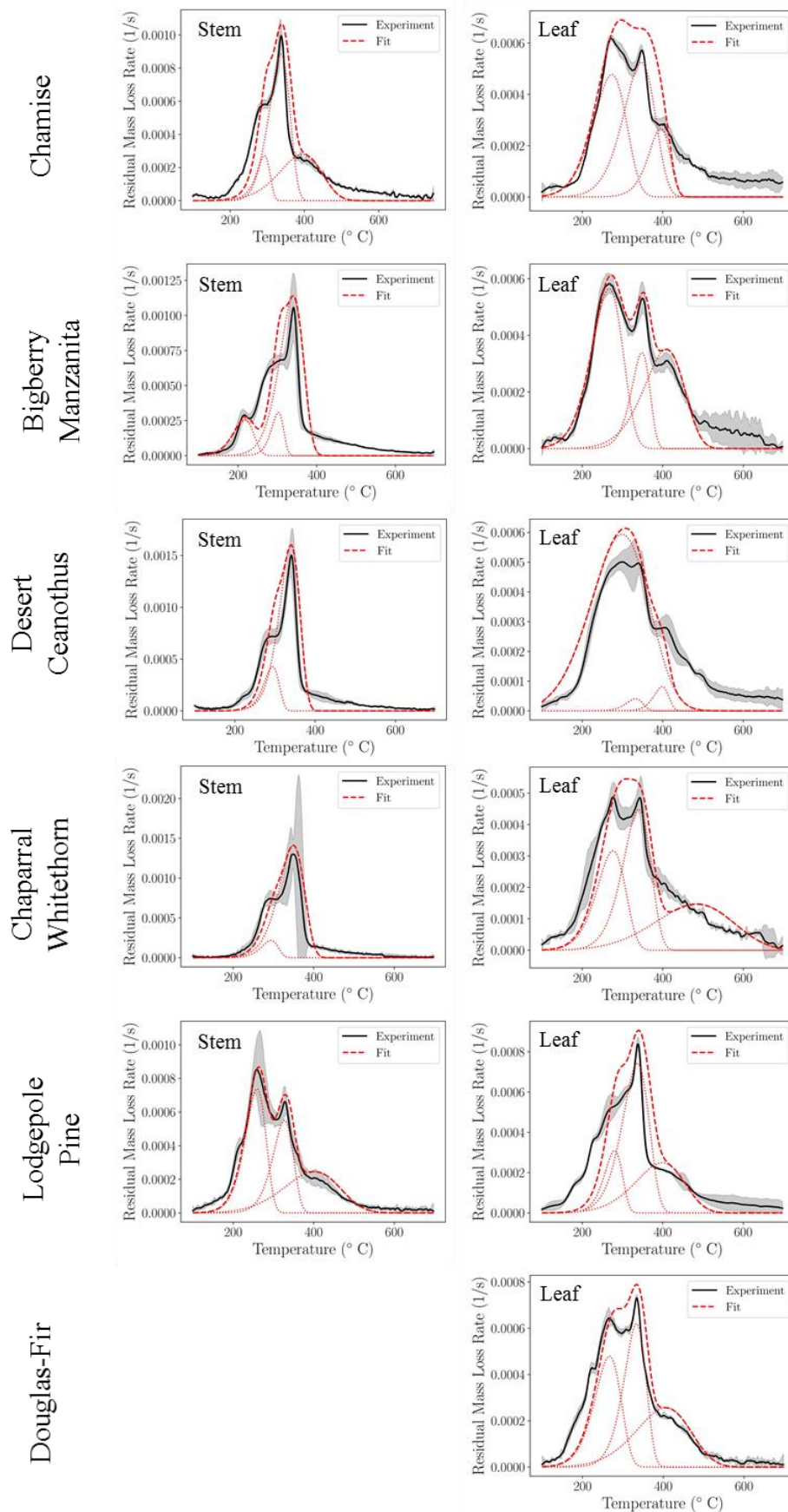
### Thermal Analysis Experiments

Figure 1 plots the results of TGA experiments conducted on stem and leaf samples of all plant species tested in this work. Solid black lines represent the mean of repeated experiments; the shaded area is calculated as one standard deviation. Also shown in Fig. 1, as red lines, are model-predictions of sample behavior during TGA experiments (dashed and dotted lines represent total and reaction-step-specific model-predicted residual mass loss rates, respectively). Optimized kinetic parameters for each of these reaction mechanisms are provided in Table 4. The details of this fitting process are provided in a related work <sup>26</sup>. As seen in Fig. 1, all models capture experimentally measured mass loss rate data with reasonable accuracy.

Table 4. Kinetic Parameters Describing Decomposition of Vegetative Fuels

Sample Name	$A_1$ (s <sup>-1</sup> )	$E_1$ (kJ kmol <sup>-1</sup> )	$\Delta m_1$	$A_2$ (s <sup>-1</sup> )	$E_2$ (kJ kmol <sup>-1</sup> )	$\Delta m_2$	$A_3$ (s <sup>-1</sup> )	$E_3$ (kJ kmol <sup>-1</sup> )	$\Delta m_3$
Leaves									
Chamise	9.98×10 <sup>2</sup>	5.67×10 <sup>4</sup>	0.30	1.21×10 <sup>4</sup>	7.69×10 <sup>4</sup>	0.32	3.39×10 <sup>8</sup>	1.37×10 <sup>5</sup>	0.11
Bigberry Manzanita	2.12×10 <sup>3</sup>	5.91×10 <sup>4</sup>	0.34	3.64×10 <sup>9</sup>	1.39×10 <sup>5</sup>	0.12	1.07×10 <sup>3</sup>	7.23×10 <sup>4</sup>	0.27
Desert Ceanothus	2.22	3.32×10 <sup>4</sup>	0.64	9.99×10 <sup>10</sup>	1.52×10 <sup>5</sup>	0.01	3.80×10 <sup>14</sup>	2.14×10 <sup>5</sup>	0.02
Chaparral Whitethorn	9.85×10 <sup>3</sup>	6.68×10 <sup>4</sup>	0.17	1.15×10 <sup>5</sup>	8.68×10 <sup>4</sup>	0.24	1.53	4.36×10 <sup>4</sup>	0.21
Lodgepole Pine	2.38×10 <sup>5</sup>	8.99×10 <sup>4</sup>	0.38	2.85×10 <sup>8</sup>	1.12×10 <sup>5</sup>	0.11	6.39×10 <sup>1</sup>	5.67×10 <sup>4</sup>	0.23
Douglas-Fir	3.35×10 <sup>4</sup>	7.07×10 <sup>4</sup>	0.24	1.45×10 <sup>7</sup>	1.09×10 <sup>5</sup>	0.26	2.13×10 <sup>1</sup>	5.17×10 <sup>4</sup>	0.26
Stems									
Chamise	9.56×10 <sup>6</sup>	1.08×10 <sup>5</sup>	0.38	3.40×10 <sup>12</sup>	1.58×10 <sup>5</sup>	0.07	1.43×10 <sup>2</sup>	6.04×10 <sup>4</sup>	0.24
Bigberry Manzanita	4.85×10 <sup>5</sup>	7.41×10 <sup>4</sup>	0.10	2.14×10 <sup>6</sup>	1.01×10 <sup>5</sup>	0.53	2.06×10 <sup>14</sup>	1.79×10 <sup>5</sup>	0.07
Desert Ceanothus	1.16×10 <sup>8</sup>	1.20×10 <sup>5</sup>	0.64	5.05×10 <sup>10</sup>	1.39×10 <sup>5</sup>	0.13			
Chaparral Whitethorn	3.23×10 <sup>9</sup>	1.26×10 <sup>5</sup>	0.07	9.56×10 <sup>5</sup>	9.86×10 <sup>4</sup>	0.69			
Lodgepole Pine	3.45×10 <sup>6</sup>	8.91×10 <sup>4</sup>	0.30	5.97×10 <sup>7</sup>	1.15×10 <sup>5</sup>	0.22	1.51×10 <sup>1</sup>	4.96×10 <sup>4</sup>	0.26
Average Stem*	8.58×10 <sup>5</sup>	9.64×10 <sup>4</sup>	0.49	1.03×10 <sup>16</sup>	1.95×10 <sup>5</sup>	0.07			
Average Leaf*	1.22×10 <sup>3</sup>	5.75×10 <sup>4</sup>	0.23	2.46×10 <sup>5</sup>	9.03×10 <sup>4</sup>	0.23	1.32×10 <sup>2</sup>	6.02×10 <sup>4</sup>	0.25

\* Effective values representing the thermal decomposition of a typical leaf or stem tested in this work



**Figure 1.** Experimentally measured and model predicted mass loss rate data of stem (left) and leaf (right) samples of Chamise, Bigberry Manzanita, Desert Ceanothus, Chaparral Whitethorn, Lodgepole Pine, and Douglas-Fir in TGA tests conducted in Nitrogen at  $10\text{ }^{\circ}\text{C min}^{-1}$ .

Temperature-resolved mass loss rate measurements obtained during TGA experiments on all vegetative fuels tested in this work are plotted together in Fig. 2, to allow for a qualitative comparison of the thermal degradation behavior of each of these fuels. As seen here, between each fuel, there are distinct differences in the onset temperature of degradation, the number of apparent reactions, and the peak measured mass loss rate (as well as the temperature at which it occurs). Across all samples tested, the temperature corresponding to each of these reaction peaks varies between 220 and 485 °C. In general, two reaction peaks (local maxima in  $\frac{d(m/m_0)}{dt}$ ) are observed for stem samples. Stem samples demonstrated higher peak mass loss rates than leaves and their decomposition generally occurred over a narrower temperature range, with little mass loss above 400 °C. Leaf samples were characterized by a series of overlapping reactions, typically at least three, that occurred over a wider temperature range. These results support previous observations by Sussot<sup>14</sup>, who noted that the relative proportions of extractives (i.e., volatile hydrocarbons), hemicellulose, cellulose, and lignin appear to explain the mg-scale thermal degradation behavior of typical forest fuels. Also plotted in this figure (black lines) are curves representing the degradation behavior of an idealized ‘Average’ stem or leaf. It should be stressed that these curves do not represent actual measurement data: rather, they define a curve representative of typical stem or leaf degradation, which is used in this work to help interpret wildfire simulation results. Kinetic parameters used to define these curves are reported in Table 4 under the sample names ‘Average Stem’ and ‘Average Leaf’.

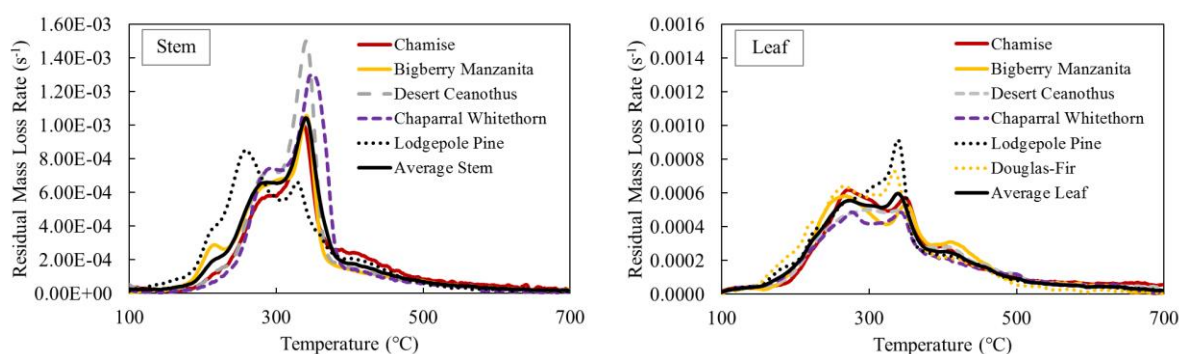


**Figure 2.** Measured mass loss rates of all vegetative fuels tested in this work when heated (in ultra-high purity nitrogen) at 10 °C min<sup>-1</sup> in the TGA. Each curve represents an average of five repeated experiments; for clarity, measurement uncertainty is not plotted (this is shown in Fig. 1).

Figure 3 plots experimentally measured heat release rate, HRR, (normalized by volatilized sample mass,  $m_{vol}$ ) of stem and leaf samples of all plant species tested in this work in the MCC. Experimental measurements are plotted as solid black lines. Measured values of  $\Delta H_{c,total}$  and  $\mu_{char}$  are reported in Table 5. Uncertainties are reported for  $\mu_{char}$  as one standard deviation and for  $\Delta H_{c,total}$  as the maximum of either: one standard deviation of repeated measurements or 5% of the average value (which represents the inherent uncertainty in oxygen consumption measurements of heat release<sup>31</sup>). Measured values of  $\Delta H_{c,total}$  vary between 8.9 14.4 kJ g<sup>-1</sup> and 14.4 kJ g<sup>-1</sup>, which is a significant deviation from the value of 18.6 kJ g<sup>-1</sup> that is prescribed for most (39 of 40) fuels in the Standard Fire Behavior Fuel Models<sup>6</sup>. For the fuels tests in this work, exclusive of Lodgepole Pine stems, measured values of  $\Delta H_{c,total}$  are, on average, 17% greater for leaves than for stems. The heat of combustion of Lodgepole Pine stems is neglected in this comparison because it is, 42% greater than the average  $\Delta H_{c,total}$  of the other stems tested in this work.

Also shown in Fig. 3 are model predictions of heat release rate (i.e., model-predicted mass loss rate, scaled by the heats of combustion,  $\Delta H_{c,i}$ ). Optimized values for  $\Delta H_{c,i}$  are presented in Table 5; these values are calculated based on the ratio of experimentally measured heat release rate (in MCC tests) and mass loss rate (in TGA tests) at the peak mass loss rate of each of the reaction steps defined by the fuel’s decomposition model (Table 4). This calculation accounts for relative fraction of gaseous volatiles produced by each reaction step at the temperature of interest. The uncertainty in reported values of  $\Delta H_{c,i}$  is estimated to be 15% based on a propagation of the 5% uncertainty in heat release

measurements and the differences between of model-predicted and experimentally-measured sample mass loss rate (see Fig. 1), which was used to generate the HRR curves shown in Fig. 3.

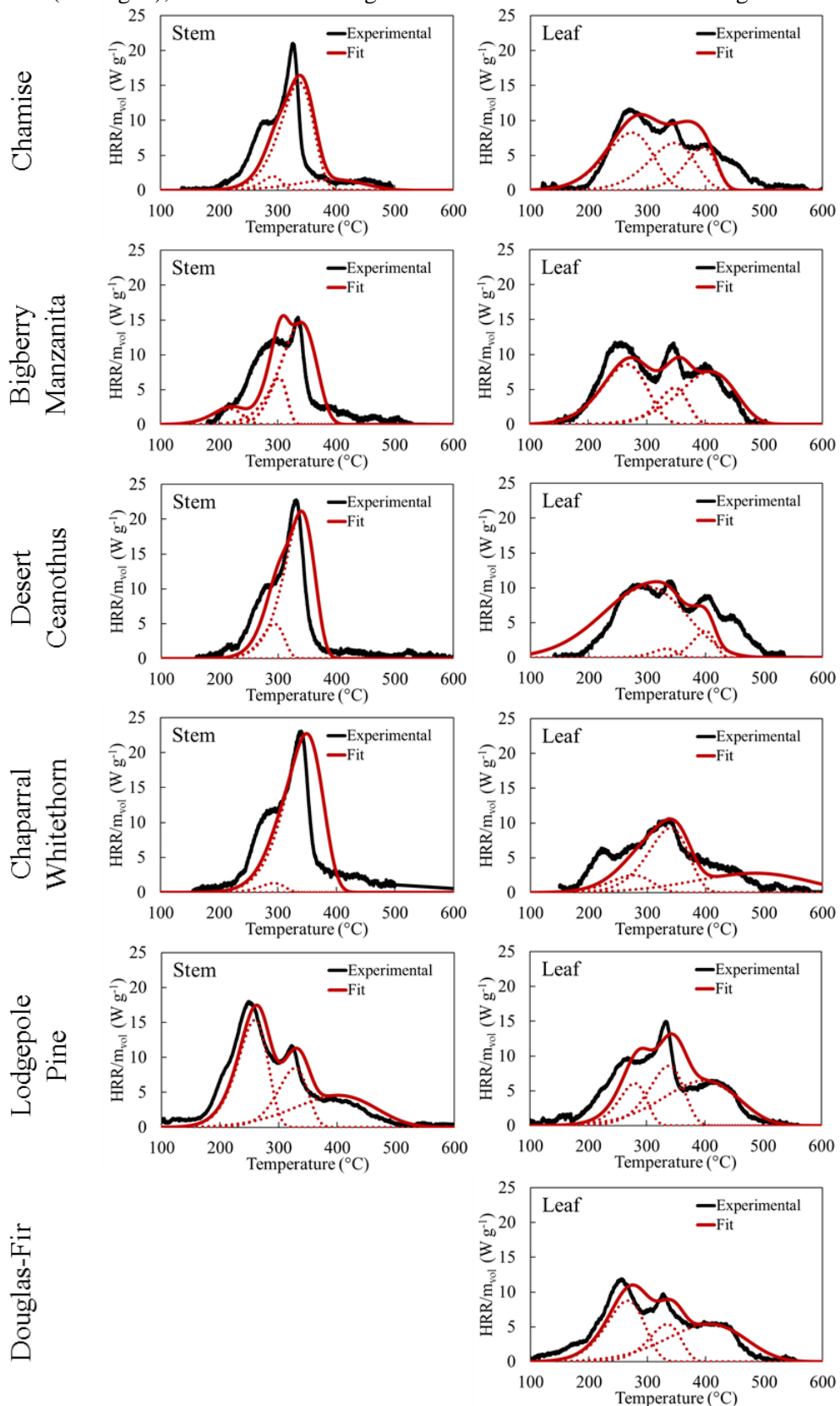


**Figure 3.** Experimentally-measured and model-predicted heat release rate of stem (left) and leaf (right) samples of Chamise, Bigberry Manzanita, Desert Ceanothus, Chaparral Whitethorn, Lodgepole Pine, and Douglas-Fir in MCC tests conducted in Nitrogen at 10 °C min<sup>-1</sup>.

Table 5. Heats of Complete Combustion and Char Yields of Vegetative Fuels

Sample Name	$\Delta H_{c,1}$ (kJ g <sup>-1</sup> )	$\Delta H_{c,2}$ (kJ g <sup>-1</sup> )	$\Delta H_{c,3}$ (kJ g <sup>-1</sup> )	$\Delta H_{c,total}$ (kJ g <sup>-1</sup> )	$\mu_{char}$ (-)
Leaves					
Chamise	17.3±2.6	12.9±1.9	22.9±3.4	11.7±1.2	0.25±0.04
Bigberry Manzanita	15.4±2.3	14.9±2.2	21.8±3.3	12.4±0.9	0.22±0.06
Desert Ceanothus	17.1±2.6	30.7±4.6	47.4±7.1	12.3±1.1	0.32±0.03
Chaparral Whitethorn	7.9±1.2	20.7±3.1	19.0±2.8	10.4±1.8	0.33±0.04
Lodgepole Pine	10.8±1.6	16.1±2.4	23.6±3.5	12.6±0.6	0.24±0.04
Douglas-Fir	18.3±2.7	8.7±1.3	21.1±3.2	12.2±0.6	0.25±0.04
Average Leaf*	-	-	-	11.9±0.8	0.27±0.05
Stems					
Chamise	17.5±2.6	7.3±1.1	5.5±0.8	8.9±0.6	0.27±0.04
Bigberry Manzanita	9.0±1.4	12.9±1.9	21.9±3.3	8.9±0.9	0.37±0.06
Desert Ceanothus	13.2±2.0	11.7±1.8		9.1±0.5	0.25±0.06
Chaparral Whitethorn	6.1±0.9	16.1±2.4		11.5±2.6	0.23±0.05
Lodgepole Pine	20.8±3.1	15.4±2.3	18.6±2.8	14.4±2.0	0.22±0.04
Average Stem*	-	-	-	10.9±2.3	0.27±0.05

\*Calculated as the mean value of  $\Delta H_{c,total}$  or  $\mu_{char}$  measured for all stem or leaf species

### Numerical Simulations of Wildfire Spread

Figure 4 plots time-resolved predictions of fire front location in FDS simulations using the decomposition models developed in this work for stems and leaves of Bigberry Manzanita, Chamise, and Chaparral Whitethorn. The fire front is defined as the location of the maximum gas temperature in a 1 m wide, 1 m tall strip along the centerline of the grass field. As seen in Fig. 4, propagation of this fire front across the length of the field occurred at a fairly constant rate,  $R$ , which varied between 0.50 and 1.09 m s<sup>-1</sup> (factor of two difference) when using the decomposition models developed in this work.

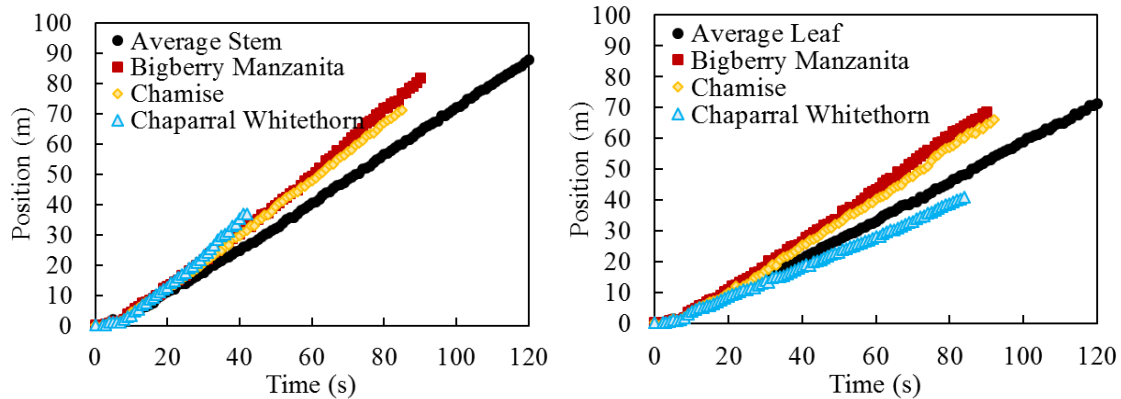


**Figure 4.** Comparison of predicted fire front position of CSIRO C064 Grassland Fires simulated in FDS 6.7.1 using the thermal decomposition models developed for three stem (left) and leaf (right) vegetative fuels tested in this work.

The calculated fire spread rates for ‘Average Stem’ and ‘Average Leaf’ models are  $R_{avg}^{stem} = 0.75$  m s<sup>-1</sup> and  $R_{avg}^{leaf} = 0.61$  m s<sup>-1</sup>, respectively (a relative difference of 24%). This indicates that measured differences in the decomposition behavior of stems and leaves (e.g., in heats of combustion or decomposition temperature, range, and peak mass loss rate) produce distinct differences in the global behavior of wildfires in FDS simulations. To better understand how well average stem or leaf models capture the behavior of fuel-specific stem or leaf models, a simple sensitivity analysis was performed.

Model sensitivity of predicted fire spread rate was calculated as  $S = \frac{(R_i - R_{avg})}{R_{avg}}$  where  $R_i$  and  $R_{avg}$  represent the fire spread rates calculated using a specific (stem or leaf) fuel model or that of the

average (stem or leaf) fuel model. Calculated sensitivity varied between 0.22 and 0.45 for the three stem species and -0.17 and 0.37 for the three leaf species simulated here. This indicates that, not only is the predicted wildfire spread rate of leaves different from that of stems, but there are distinct differences between the predicted fire spread rates of individual fuels of the same type.

## CONCLUSIONS

In this work, the thermal degradation behavior of stem and leaf samples of six vegetative fuels commonly found in the United States was examined through a series of thermogravimetric analysis (TGA) and microscale combustion calorimetry (MCC) experiments. Measurement data from TGA experiments was used to determine effective thermal decomposition mechanisms – consisting of a series of parallel, first order, Arrhenius rate reactions – and associated kinetics. MCC experiments were repeated under the same experimental conditions as TGA tests, thus allowing for the determination the heats of complete combustion of all gaseous pyrolyzates released by the degrading sample,  $\Delta H_{c,total}$ , and heats of complete combustion of the gases species produced during each reaction step,  $\Delta H_{c,i}$ . MCC data was also used for the validation of the decomposition mechanisms and species char yields,  $\mu_{char}$ , determined from TGA experiments.

Distinct differences were measured in the onset temperature of degradation, the number of apparent reactions, and the peak measured mass loss and heat release rates (as well as the temperatures at which they occur). Across all samples tested, the temperatures corresponding to the peaks of each reaction step in the determined degradation mechanisms varied by more than 250 °C. In general, stem samples demonstrated higher peak mass loss rates than leaf samples and their decomposition generally occurred over a narrower temperature range, with little mass loss above 400 °C. Leaf samples were characterized by a series of overlapping reactions that occurred over a wider temperature range and generally had higher heats of combustion. FDS simulations were run to examine the sensitivity of model predictions of wildfire spread rate to these measured variations in the thermal decomposition behavior of these fuels. Six fuel models were selected for this sensitivity analysis: simulations demonstrated a clear dependence on fuel decomposition mechanism, with predictions of wildfire spread rate varying between 0.50 m s<sup>-1</sup> and 1.09 m s<sup>-1</sup>.

## ACKNOWLEDGEMENTS

The authors would like to thank Dr. Sara McCallister of the Rocky Mountain Research Station and Dr. David Weise of the Pacific Southwest Research Station for collecting and sharing the vegetative fuel samples tested in this work and for helpful discussions during the planning stages of this project. Preliminary TGA experiments and related analysis were conducted at NIST by David Hoddinott; the authors are grateful for his assistance. Wildfire simulations and a final review of this manuscript were assisted by Dr. Kevin McGrattan of NIST – this was greatly appreciated, especially given the condensed timeframe in which this help was offered.

## REFERENCES

1. Government Accountability Office (GAO), “Technology Assessment: Protecting Structures and Improving Communications During Wild-Land Fires,” Technical Report GAO-05-380, United States Government Accountability Office: Washington, DC. (2005)
2. National Interagency Fire Center (NIFC). Total wildland fires and acres, 1983–2017. Accessed October 2018. [www.nifc.gov/fireInfo/fireInfo\\_stats\\_totalFires.html](http://www.nifc.gov/fireInfo/fireInfo_stats_totalFires.html).
3. Heinsch, F. A., Andrews, P.L., “BehavePlus fire modeling system version 5.0: Design and Features,” Gen. Tec. Rep., RMRS-GTR-249, US Department of Agriculture, Rocky Mountain Research Station, Fort Collins, CO. (2010)
4. Finney, M. A., “FARSITE: Fire Area Simulator – Model Development and Evaluation,” RMRS-RP-4, US Department of Agriculture, Rocky Mountain Research Station, For Collins CO. (2004)
5. Rothermel, R. C., “A Mathematical Model for Predicting Fire Spread in Wildland Fuels,” USDA Forest Service, Intermountain Forest and Range Experiment Station, Research Paper INT-115. (1972)

6. Scott, J.H., Burgan, R.E., "Standard Fire Behavior Fuel Models: A Comprehensive Set for Use with Rothermel's Surface Fire Spread Model," RMRS-GTR-153, US Department of Agriculture, Rocky Mountain Research Station, Fort Collins, CO. (2005)
7. Finney, M. A., Cohen, J.D., McAllister, S.S., Jolly, M., "On the Need for a Theory of Wildland Fire Spread," *International Journal of Wildland Fire* 22: p. 25-36. (2013)
8. Mell, W., Jenkins, M.A., Gould, J., Cheney, P., "A physics-based approach to modeling grassland fires," *International Journal of Wildland Fire* 16: p. 1-22. (2007)
9. McGrattan, K.B., "Progress in Modeling Wildland Fires using Computational Fluid Dynamics," 10<sup>th</sup> US Combustion Meeting, College Park, MD. (2017)
10. Gollner, M., Trouvé, A., "Towards Data-Driven Operational Wildfire Spread Modeling," WIFIRE Workshop, San Diego, CA. (2015)
11. Philpot, C.W., "Influence of Mineral Content on the Pyrolysis of Plant Materials," *Forest Science* 16: p. 461-471. (1970)
12. Shafizadeh, F., "Introduction to Pyrolysis of Biomass," *Journal of Analytical and Applied Pyrolysis* 3: p. 283-305. (1982)
13. Sussot, R. A., "Thermal Behavior of Conifer Needle Extractives," *Forest Science* 26: p. 347-360. (1980)
14. Sussot, R. A., "Characterization of the Thermal Properties of Forest Fuels by Combustible Gas Analysis," *Forest Science* 28: p. 404-420. (1982)
15. Sussot, R. A., "Differential Scanning Calorimetry of Forest Fuels," *Forest Science* 28: p. 839-851. (1982)
16. Rogers, J.M., Sussot, R.A., Kelsey R.G., "Chemical Composition of Forest Fuels Affecting Their Thermal Behavior," *Canadian Journal of Forest Research* 16: p. 721-726. (1986)
17. Dimitrakopoulos, A.P., "Thermogravimetric Analysis of Mediterranean Plant Species," *Journal of Analytical and Applied Pyrolysis* 60: p. 123-130. (2001)
18. Statheropoulos, M., Liodakis, S., Tzamtzis, N., Pappa, A., Kyriakou, S., "Thermal Degradation of Pinus Halepensis Pine-Needles Using Various Analytical Methods," *Journal of Analytical and Applied Pyrolysis* 43: p. 115-123. (1997)
19. Safdari, M-S., Rahmati, M., Amini, E., Howarth, J.E., Berryhill, J.P., Dietsberger, M., Weise, D.R., Fletcher, T.H., "Characterization of pyrolysis products from fast pyrolysis of live and dead vegetation native to the Southern United States," *Fuel* 229: p. 151-166. (2018)
20. Amini, E., Safdari, M-S., DeYoung, J.T., Weise, D.R., Fletcher, T.H., "Characterization of pyrolysis products from slow pyrolysis of live and dead vegetation native to the Southern United States," *Fuel* 235: p. 1475-1491. (2019)
21. McAllister, S., Finney, M., "Convection Ignition of Live Forest Fuels," *Fire Safety Science* 11: p. 1312-1325. (2014)
22. NETZSCH, "Software Manual (STA 449 F1 & F3) Temperature and Sensitivity Calibration," Wittelsbacherstrasse 42, 95100 Selb, Germany: NETZSCH Gerätebau GmbH. (2012)
23. Lyon, R.E., Safronava, N., Senese, J., Stoliarov S.I., "Thermokinetic model of sample response in nonisothermal analysis," *Thermochimica Acta* 545: 82-89. (2012)
24. Vyazovkin, S., Chrissafis, K., Di Lorenzo, M.L., Koga, N., Pijolat, M., Roduit, B., Sbirrazzuoli, N. Sunol, J.J., "ICTAC Kinetics Committee Recommendations for Performing Kinetic Computations on Thermal Analysis Data," *Thermochimica Acta* 590: p. 1-23. (2014)
25. Stoliarov S.I., Li J., "Parameterization and Validation of Pyrolysis Models for Polymeric Materials; *Fire Technology* 52: p. 79-91. (2016)
26. Bruns, M.C., Leventon, I.T., "Automated Fitting of Thermogravimetric Analysis Data," *Interflam 2019*
27. ASTM D7309, "Standard Test Method for Determining Flammability Characteristics of Plastics and Other Solid Materials Using Microscale Combustion," ASTM International: West Conshohocken, PA, USA. (2013)
28. Lyon, R. E., Walters, R. N., Stoliarov, S. I., Safronava, N., "Principles and Practice of Microscale Combustion Calorimetry," FAA Report, DOT/FAA/TC-12/53 R3 (April 2013)
29. McGrattan, K., Hostikka, S., McDermott, R., Floyd, J., Vanella, M., "Fire Dynamics Simulator Technical Reference Guide," NIST Special Publication 1018-1, Sixth Edition. (2019)
30. Cheney, N.P., Gould, J.S., Catchpole, W.R., "The Influence of Fuel, Weather and Fire Shape Variables on Fire-Spread in Grasslands," *International Journal of Wildland Fire* 3: p. 31-44, 1993.
31. Hugget, C. "Estimation of Rate of Heat Release by Means of Oxygen Consumption Measurements," *Fire and Materials* 4: p. 61-65. (1980)